# Structure and Composition of Air Shower Cores*

HAROLD L. KASNITZ AND KURT SITTE
*Department of Physics, Syracuse University, Syracuse, New York*
(Received June 24, 1953; revised manuscript received October 14, 1953)

Extensive air showers were observed with an arrangement in which details of their structure and composition could be studied with the help of a large cloud chamber and a 102-counter hodoscope, while extension trays permitted a classification of the showers in three groups according to their initial energy, and a selection favoring events with cores striking near the central cloud chamber-hodoscope set. The electron density distribution is found to be flatter than the Molière structure function, and despite the different shower ages in the three energy groups, to be nearly the same for all the showers recorded. A structure function $\phi(r) \propto r^{-0.76}$ to $r^{-0.85}$ in the immediate neighborhood of the core fits the data best. An attempt to correlate the very dense local cascades started by high-energy electrons or photons with the expected multiple cores representing the high multiplicity of the nuclear interaction initiating the shower failed; the structure of the groups of local cascades observed does not appear to vary with the shower energy. The penetrating component contains $N$ particles interacting in the lead plates of the chamber with a mean free path of approximately 165 g/cm$^2$, and consisting of neutrons (41±8 percent) and charged particles. The total abundance of penetrating particles near the core does not differ appreciably from that found by various authors in experiments not as strongly biased in favor of the detection of shower cores. The abundance ratios of $N$ particles to $\mu$ mesons, and of penetrating particles to electrons, show only slight variations with the shower age and demonstrate that the nucleonic cascade reaches its maximum somewhat later than the electron cascade.

## I. INTRODUCTION

IT has frequently been stressed as a remarkable fact that the theory of cascades initiated by a single particle, when applied to the description of air shower phenomena, is successful although the process of the development of an extensive shower is of a greatly more complicated nature. It has also been recognized that this success is not really fortuitous, but a result of the circumstance that many of the features of electron cascades are essentially determined by the properties of the shower within a few cascade units from the point of observation, and thus independent of the initial development of the cascade as long as the observation is restricted to a region not including the shower axis and its immediate surrounding, the shower core. It is only in this region that the nature of the initiating process strongly affects the shower structure, and that deviations from the classical single-particle cascade theory have been observed. The density distribution, as investigated by various authors (e.g., Williams,[1] Prescott and Campbell,[2] Hazen,[3] Williams and Hazen[4]) is flatter than that calculated by Molière[5] for a cascade initiated by a single particle.

In most cases, however, the analysis has suffered from a surfeit of variables. In particular in counter experiments, showers of all energies—or more correctly, of all particle numbers—were recorded indiscriminately, with detection systems which were rather insensitive to the accurate location of the shower axis. Thus, an analysis averaging over density spectrum, lateral distribution—both presumably depending on the age of the shower—and core location could scarcely be expected to yield an unambiguous picture of the details of the initial distribution.

It seemed therefore worthwhile to perform an experiment with a technique improved in two respects: firstly, by using an arrangement which rejects more strongly events in which the shower core strikes at an appreciable distance from the apparatus and which consequently more stringently registers shower cores; and secondly, by recording—at least within reasonable limits—the total number of shower particles, and therefore classifying the showers as to their average age. A study of the electron density distribution under these controlled conditions, together with a study of penetrating particles in the core region, can be expected to reveal some additional pertinent information on the nature of the process in which extensive showers originate and by which they propagate.

## II. THE EXPERIMENTAL ARRANGEMENT

### (1) Description

The experimental arrangement consisted of a shower selector set ("masterpulse set") and a "core analyzer." The shower selector was made up of three pairs of counter trays and two large single counters placed at the center of the arrangement. Each tray contained ten counters; those in the $A$ trays had an active area of 1 in.×16 in., while the $B$ and $C$ counters were of 1 in.×12 in. active area. The three sets of trays were situated symmetrically with respect to the core analyzer, as shown in the schematic drawing of Fig. 1(a), with

* Supported in part by the U. S. Atomic Energy Commission. Part of this work is included in the paper submitted by one of us (H.L.K.) as a Ph.D. thesis at Syracuse University.
[1] R. W. Williams, Phys. Rev. **74**, 1689 (1948).
[2] I. D. Campbell and J. R. Prescott, Proc. Phys. Soc. (London) (London) **A65**, 258 (1952).
[3] W. E. Hazen, Phys. Rev. **85**, 455 (1952).
[4] R. W. Williams and W. E. Hazen, Phys. Rev. **90**, 361 (1953).
[5] G. Molière in *Cosmic Radiation*, edited by W. Heisenberg (Springer Verlag, Berlin, 1943, and Dover Publications, New York, 1946).

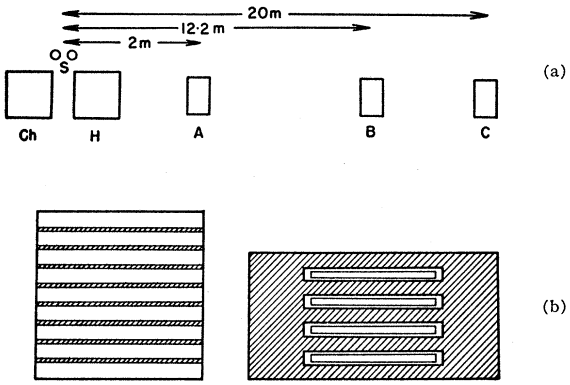


FIG. 1. The experimental arrangement. (a) General layout: Cloud chamber (Ch), hodoscope (H) and three of the six counter trays. (b) The analyzer set: 24-in. square cloud chamber with eight ½-in. lead plates, and hodoscope of four counter trays in lead pile.

the $A$ trays at a distance of 2 m, the $B$ trays at 12.2 m, and the $C$ trays at 20 m from the center. Each of the central counters $S$ had an active area of 2 in.×24 in.

Three different masterpulses were formed, dividing all of the recorded showers into three groups as follows:

(i) At least two counters struck in each of the $A$ trays, less than two counters struck in each of the $B$ trays, and both central counters $S$ triggered ("$A$ showers");

(ii) At least two counters struck in each of the $B$ trays, less than five counters struck in each of the $C$ trays, and both central counters struck ("$B$ showers");

(iii) At least five counters struck in each of the $C$ trays, and both central counters triggered ("$C$ showers").

This triggering system imposed on the events selected at least a rough symmetry with respect to the core analyzer situated at the center, and, because of the anticoincidence arrangement, was strongly biased in favor of showers whose axes struck near the center. It may be noted that the $S$ counters affect the selection only in a very small degree, but they reduce the chance coincidence rate very appreciably.

Diode clippers were used in the masterpulse circuits, and after reduction to uniform height the counter pulses were fed through diode isolating circuits to an integrating circuit. The output of the integrator was amplified by a 12AU7 located at each tray, and fed through a cathode follower to a 6AK5 discriminator. A setting of each tray discriminator allowed the selection of outputs corresponding to two or more, or five or more, counters simultaneously discharged. The appropriate coincidence and anticoincidence circuits, actuated by the outputs of the six tray discriminators and the outputs of the two counters $S$, formed the masterpulses. As a check on the performance of the triggering system, each tray discriminator and the three masterpulse arrangements separately triggered a thyratron. Whenever a shower was recorded, neon lights were photographed indicating both the type of masterpulse and the trays hit. For instance, for an $A$ shower only the $A_1$ and $A_2$ lights should be seen, together with the $A$ masterpulse light.

The analyzer set consisted of a large cloud chamber (24 in.×24 in.×10 in.) fitted with eight ½-in. lead plates, and a hodoscope arrangement of 102 counters arranged in four trays of 20, 24, 28, and 30 counters, respectively. The two upper trays contained counters of 1 in.×12 in. size, the two lower trays 1 in.×16 in. counters. The trays were separated from each other by layers of 2-in. lead, and shielded by 8-in. lead walls from the sides and 2-in. lead on top. Cloud chamber and hodoscope were placed side by side as close as possible to each other. As in an earlier experiment[6] the coordination of the two instruments was simplified by a system of clocks, double registers, and neon indicators.

The analyzer set is schematically shown in Fig. 1(b). It offers the advantage not only of a large area (about 0.25 m²) usable for analysis, but also of observation over a considerable range of penetration. In the hodoscope set the shower development can be followed through a total of 8 in. of lead absorber, and the data in the upper hodoscope tray can be reduced to incident densities with the help of the observations of the transition effect in 2 in. of Pb seen in the chamber. This feature is particularly useful for the study of the penetrating shower component.

A total of about 1300 cloud-chamber photographs and more than 2800 hodoscope records were analyzed. Hodoscope pictures without a corresponding chamber photograph, taken during the recycling period of the cloud chamber or belonging to events where the chamber picture was not considered good enough for full analysis, where still of value for the statistical analysis discussed below.

### (2) Discussion of the Triggering Arrangement

It is always useful in an air shower experiment, and necessary for the present one, to analyze the performance of the triggering arrangement. In particular, to substantiate the claims made in Sec. I, the selectivity of the masterpulse system as to shower size and location must be evaluated.

For this calculation the following two customary assumptions have been made:

(i) That the lateral distribution of the shower is represented by the Bethe approximation[7] to the Molière structure function

$$f(r)=\frac{c}{r}(1+4r)\exp(-4r^{2/3}), \tag{2.1}$$

where $c$ is a constant and $r$ the distance from the core measured in shower units. The limitation of the

[6] Froehlich, Harth, and Sitte, Phys. Rev. 81, 504 (1952).
[7] H. A. Bethe, Phys. Rev. 59, 684 (1941).

validity of the Bethe approximation to comparatively small distances $r$ is of no concern since the triggering arrangement efficiently rejects events striking at too large distances from the center.

(ii) That the differential size distribution of the showers can be represented by

$$s(N)dN=KN^{-(\gamma+1)}dN, \tag{2.2}$$

with a constant $\gamma\approx 1.5$ for the entire range of efficient detection. It will be seen that this should certainly hold for the $A$ and $B$ showers which contain on the average less than $10^6$ particles, while a correction is needed for $C$ showers.

It will further be assumed that the detection efficiencies of the trays are unity, and that other corrections such as that for the finite resolving time are likewise negligible. These assumptions are of course not quite correct, but will introduce no appreciable error since only relative rates will be considered and not their absolute values.

The calculations follow the well-known pattern (e.g., Ise and Fretter,[8] Singer[9]) and only a few essential points will be repeated here. Denoting by $r_S$, $r_{A1}$, $r_{A2}\cdots$ the distances (in shower units) of the central counters, the $A_1$ tray, the $A_2$ tray, and so on, from the axis of the shower, by $\theta$ the azimuthal angle of the shower axis measured from the line connecting the trays, and by $S$, $AS$, $BS$, $CS$ the areas of the central counters and of the single $A$, $B$, and $C$ counters, respectively, one has, for instance, for the rate of $A$ showers:

$$R_A=\int_0^\infty KN^{-(\gamma+1)}dN\int_0^\infty 2\pi r dr\int_0^{\pi/2}\{[p_S(r_S,NS)]^2\times\sum_{i=2}^{n}p_A(i,r_A,ANS)\sum_{j=2}^{n}p_A(j,r_A,ANS)\times\sum_{k=2}^{n}p_B'(k,r_B,BNS)\sum_{l=2}^{n}p_B'(l,r_B,BNS)\}d\theta, \tag{2.3}$$

where the functions $p(i,r,NS)$ are the exponential expressions for the probability of a shower of $N$ particles hitting in a distance $r$ to trigger exactly $i$ out of $n$ ($=10$) counters, and the $p'$'s similarly are the probabilities of the shower missing. Thus, for instance,

$$p(i,r_A,ANS)=\{1-\exp[-ANSf(r_{A1})]\}^i\cdot\exp[-(n-i)ANSf(r_{A1})]. \tag{2.4}$$

Similar expressions are obtained for the rates of $B$ and $C$ showers.[10]

The next step in the evaluation is the compution of the triggering probability $I(r,NS)$ due to all showers striking at a distance $r$ from the central counters, as a function of the particle number $N$:

$$I_A(r,NS)=r\int_0^{\pi/2}\{p_S^2\sum_i p_{A1}\sum_j p_{A2}\times\sum_k p_{B1}'\sum_l p_{B2}'\}d\theta. \tag{2.5}$$

(The arguments in the expressions of the type (2.4) are omitted.) From it two important functions can be obtained.

(a) By integrating over $N$, one finds the contribution $P(r)$ to the recorded rates by showers of all sizes as a function of the distance $r$ of their axis from the center of the arrangement

$$P(r)=\int_0^\infty KN^{-(\gamma+1)}I(r,NS)dN. \tag{2.6}$$

The result is shown in Fig. 2. It should be noted that 50 percent of all $A$ showers strike within a radius of less than 2.5 m. The selectivity is less perfect for the $B$ showers with a maximum contribution at about 7 m, and least for $C$ showers (maximum at about 13 m). However, it will be seen later that even for those two types of events an analysis of the core structure can be obtained.

(b) By integrating over $r$, the contributions $F(N)$ to the recorded rates by showers of various particle numbers striking at all distances $r$ from the central counters are found:

$$F(N)=2\pi KN^{-(\gamma+1)}\int_0^\infty I(r,NS)dr. \tag{2.7}$$

Figure 3 summarizes the result for the three shower types. It is seen that the selection is remarkably sharp; the $A$-shower curve, for instance, is centered about

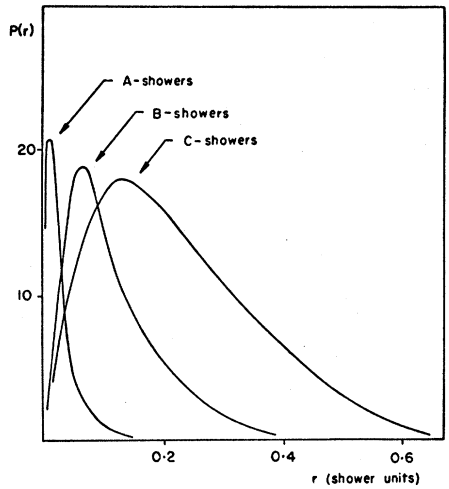


FIG. 2. The contributions $P(r)$ to the recorded rates by showers of all sizes, as a function of the distance $r$ of their axis from the center of the arrangement, for $A$, $B$, and $C$ showers.

[8] J. Ise, Jr., and W. B. Fretter, Phys. Rev. **76**, 932 (1949).
[9] S. F. Singer, Phys. Rev. **81**, 579 (1951).
[10] The very slight dependence of the probabilities $p$ and $p'$ on the zenith angle of the shower axis can be neglected in the following considerations.

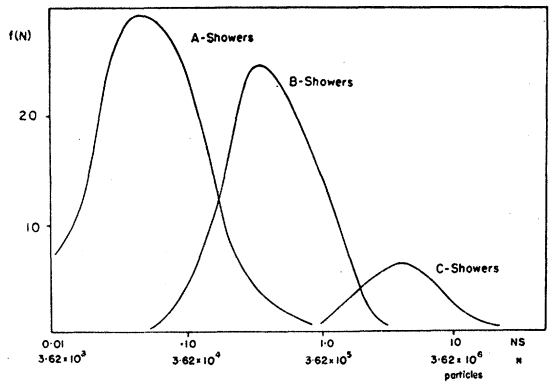


FIG. 3. The contributions $F(N)$ to the recorded rates by showers of various particle numbers $N$ striking at all distances from the center, for $A$, $B$, and $C$ showers.

$NS=0.05$ (corresponding to $N=1.81\times10^4$, or an incident energy of $0.91\times10^{14}$ ev for a single-photon initiated cascade). Its width at half-maximum is about 10, from $NS=0.018$ to $NS=0.16$. Similarly, the $B$ masterpulse selects predominantly events between $NS=0.18$ and $NS=1.5$, or from an energy interval centered about $E_0=0.71\times10^{15}$ ev, while the $C$ showers lie mostly between $NS=1.8$ and $NS=10$, with an average $E_0=0.80\times10^{16}$ ev. It is clearly seen that the separation of shower energies is satisfactorily achieved.

## III. THE ELECTRON COMPONENT

### (1) Density Distribution at the Center

Since the preceding discussion has shown that the requirements of energy classification and of core selection are fairly well met, the density distribution observed in the analyzer set can be expected to exhibit the properties of the structure function near the core as a function of the energy. Using the expressions quoted above for the triggering probabilities, and the Molière-Bethe structure function, one can calculate the frequency of events of a density $\Delta$ at the point of observation. Deviations from the theoretical curve can then be used to obtain a corrected structure function which should be compared with that derived from an improved theory. Thus the results could, in principle, yield better values for some of the parameters of shower theory and of the theory of high-energy nuclear collisions. At the present stage, however, a more modest goal should be set: The exact theory of large air showers involves not only the number, the angular distribution, and the energy spectrum of the electron-producing particles ejected in the initial collision, but also a source function representing the continuous replenishment of the electron component from the nuclear cascade. The number of adjustable parameters in the theoretical results is, therefore, so large and the correlation between structure function and basic features of the theory so far from unique, that unambiguous conclusions can scarcely be reached from the data of a single experiment. In other words, uncertainties in fundamental points make it appear premature to attempt a direct comparison between experiment and a more refined theory, although the mathematical methods of shower theory have recently been developed in a rather general form.[11] But even in carrying the analysis of the experimental data only to the point of deriving empirical corrections to the Molière-Bethe theory, one can hope to gain at least semiquantitative evidence on the relative importance of some of these fundamental features.

Both cloud-chamber and hodoscope records were used for the study of the electron density distribution. In the cloud chamber analysis, the particle numbers recorded in the pictures had to be corrected for the transition effect in the brass walls of the chamber. Bethe's multiplication factor $[1+2(1-7.2/Z)t/X_0]$ as quoted by Williams[1] was used ($Z$ is the atomic number, and $t/X_0$ the thickness in radiation lengths, of the wall material traversed), and the incidence of an equal number of photons and electrons was assumed. As Hazen has pointed out,[3] this last assumption is somewhat uncertain, but the effect is small and the possible errors involved probably negligible. A further correction of the cloud-chamber data was made for electrons not connected with the shower, but crossing the apparatus within the resolving time of the chamber. Their average number was obtained from a careful survey of the data taken with the same chamber and at the same location, but with a different triggering arrangement which demanded the incidence of an unaccompanied penetrating particle.[6]

In the analysis of the hodoscope data, two corrections were needed in order to determine the electron density of the incident air shower from the number of counters struck in the top tray. Firstly, the average number of particles present is always larger than the number of counters discharged. A correction for this effect is easily obtained if random distribution of the shower particles over the tray area can be assumed, so that the Poisson formula can be applied to express the probability that exactly $n$ counters will be hit by a shower of $m$ particles. Secondly, a statistical correction must be made for the transition effect in the 2-in. top lead absorber. For this purpose, the transition effect in the lead plates of the chamber was determined, and the data giving the average number of electrons observed under the fourth of the $\frac{1}{2}$-in. plates as a function of the number of incident electrons were then used to find the true incident density from the number of hodoscope counters struck.

The incident density distribution may be calculated assuming the Molière-Bethe structure function to be valid. Since a shower of density $\Delta$ at the center of the arrangement, whose axis strikes at a distance $r$ from

[11] E.g., L. Jánossy and H. Messel, Proc. Roy. Irish Acad. **A54**, 245 (1951); H. Messel, Proc. Phys. Soc. (London) **A64**, 726 (1951); H. S. Green and H. Messel, Phys. Rev. **88**, 331 (1952).

the center, must contain, on the average, a number $N=\Delta/f(r)$ particles, the frequency with which this event will be observed is given by

$$h(\Delta)=2\pi\Delta^{-\gamma}\int_0^\infty \{f(r)^\gamma\}I(r,\Delta S/f(r))dr. \quad (3.1)$$

For the comparison with the experiment, the integral frequency distribution $H(\Delta)$, that is, the frequency of showers of a central density $\geq\Delta$, is preferred:

$$H(\Delta)=\int_\Delta^\infty h(\Delta)d\Delta. \quad (3.2)$$

The evaluation of (3.1) and (3.2) has to be done by numerical integration. $h(\Delta)$ is first constructed by computing for various fixed $\Delta$ the contribution from showers incident at various distances, and this procedure yields some interesting auxiliary results. Thus, as it is seen from Fig. 4(a)–4(c), while $A$ showers of practically all central densities strike in the immediate neighborhood of the analyzer set, for $B$ showers this is true only when the central density exceeds about 50 particles/m$^2$, and for $C$ showers only for large showers of more than 400 particles/m$^2$ at the center. Small $B$ showers and an appreciable fraction of the $C$ showers will therefore not reveal features characteristic of the core region. On the other hand, the curves of Fig. 4(a)–4(c) show in which density region the observations will refer to true shower cores. It may be noted that, although the number of *events* in which the shower axis strikes at some distance from the analyzer becomes considerable for $C$ showers, the fraction of *particles* observed in these events in cloud chamber and hodoscope is not equally large since the "true" cores generally are the denser showers. A statistical analysis of the shower particles, as it is presented below, is therefore more strongly biased in favor of shower cores than those curves may indicate.

The integral density distributions (3.2) for the three types of showers, calculated with the Bethe structure function (2.1) for the three triggering arrangements used, are shown in Fig. 5(a)–5(c) together with the experimental observations in both the cloud chamber (circles) and the hodoscope (crosses). Clearly the theoretical results are a very poor representation of the data. It was therefore decided to improve the agreement by modifying the structure function in (3.1).

Since for small values of $r$ the Bethe function is well approximated by a $r^{-1}$ law, a power law with a changed exponent would appear the logical choice for the corrected structure function. In order to avoid pure guessing, the following procedure was used: It is assumed that the corrected structure function is of the form

$$\phi(r)=Ar^\epsilon f(r), \quad (3.3)$$

where $f(r)$ is again the Bethe function of (2.1), and $\epsilon$ a small quantity. It is then evident that using $\phi(r)$ instead of $f(r)$ for the calculation of the rates $h(\Delta)$ and $H(\Delta)$ will have a small effect on the triggering probabilities $I(r,NS)$ and a much more pronounced effect on the terms $(\Delta/f)^{-\gamma}$ as compared with $(\Delta/\phi)^{-\gamma}$

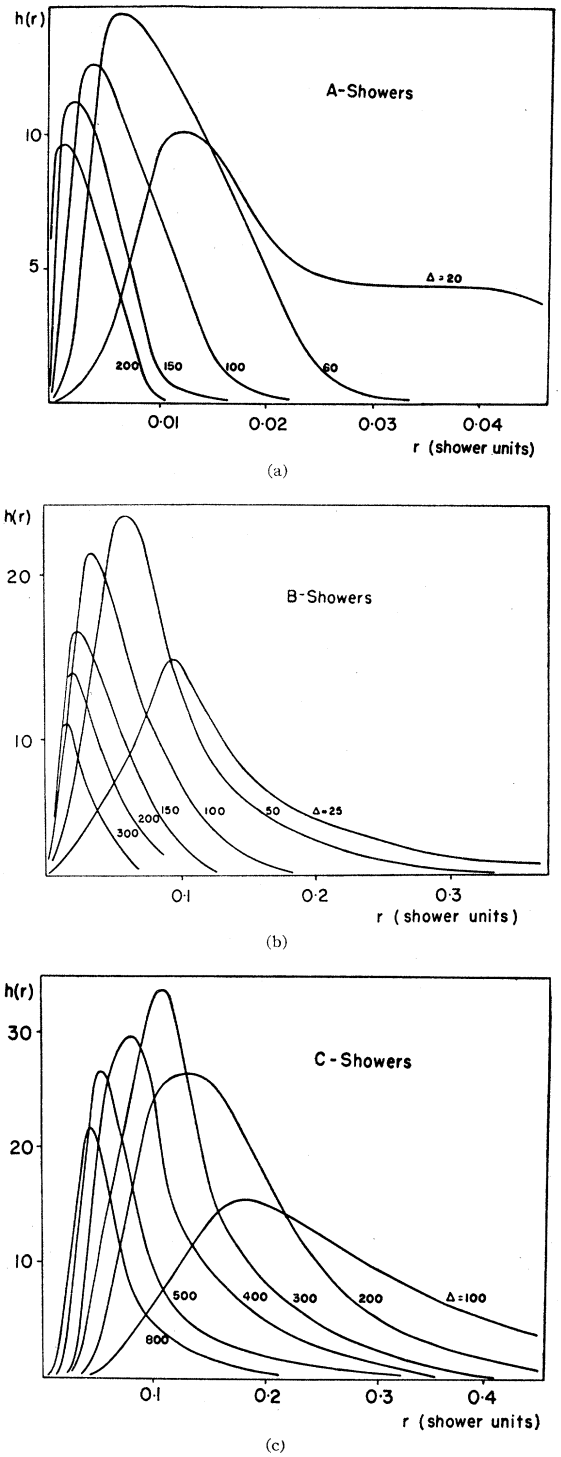


FIG. 4. Differential density distribution $h(\Delta)$ at the center of the arrangement, calculated with the Bethe structure function.

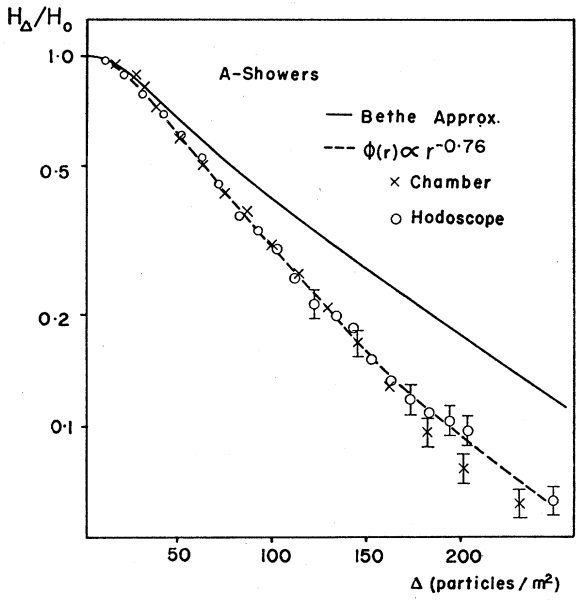


FIG. 5 (a)

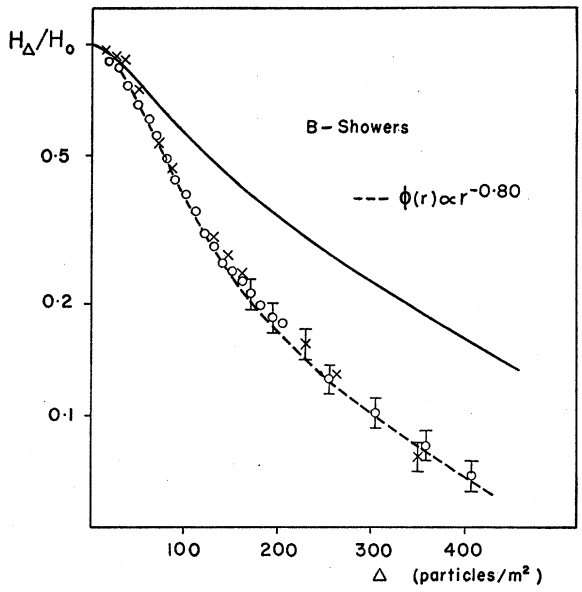


FIG. 5 (b)

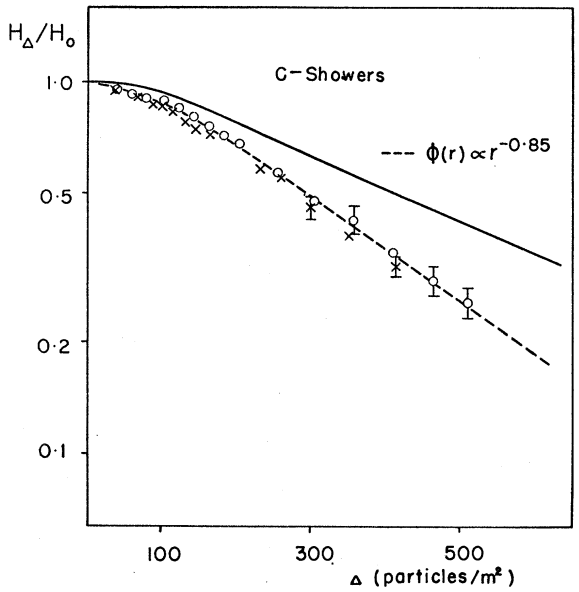


FIG. 5 (c)

FIG. 5. Integral density distribution $H(\Delta)$ at the center of the arrangement, calculated with the Bethe structure function (full line), and calculated according to (3.3) with the best $\epsilon$ (dashed line). Circles: cloud-chamber data; crosses: hodoscope data.

$=r^{\epsilon\gamma}(\Delta/f)^{-\gamma}$. Consequently it is possible to neglect the effect on $I$, and to write for the corrected differential density distribution $h'(\Delta)$:

$$h'(\Delta)=2\pi\Delta^{-\gamma}A\int_0^\infty r^{\epsilon\gamma}\{f(r)\}^\gamma I(r,\Delta/f(r))dr. \quad (3.4)$$

Moreover, in the integral the first factor $r^{\epsilon\gamma}$ is slowly varying with $r$, in comparison with $\{f(r)\}^\gamma$, so that as a first approximation it can be replaced by the constant $(R_\Delta)^{\epsilon\gamma}$, where $R_\Delta$ is the radius from which the maximum contribution derives for a given density $\Delta$. These values can be taken from the graphs of Fig. 4(a)–4(c).

Thus, by comparing the experimentally determined frequency ratio for several densities (in the region where the contribution of true cores is large) with those calculated according to (3.1) or (3.2), an average value for the constant $\epsilon\gamma$ is obtained. With this value the density distribution (3.4) was then recomputed, assuming that the modified structure function would hold exactly up to a core distance of $4m$, and joining it smoothly between 4 and $6m$ to the uncorrected Bethe function.[12] The dashed curves in Fig. 5(a)–5(c) were obtained in that way. They correspond to the following values of $\epsilon$, and structure functions

For $A$ showers: $\epsilon=0.24\pm0.02$; $\phi(r)\propto r^{-(0.76\pm0.02)}$

for $B$ showers: $\epsilon=0.20\pm0.02$; $\phi(r)\propto r^{-(0.80\pm0.02)}$

for $C$ showers: $\epsilon=0.15\pm0.04$; $\phi(r)\propto r^{-(0.85\pm0.02)}$.

$C$ showers showed, however, also another important deviation. Although the effect of the core structure function should be noticeable only for $\Delta\gtrsim400$ particles/m², the agreement between experimental and calculated values was poor even for smaller showers. The reason for this deviation is that even the $C$ showers with small densities at the center of the apparatus still contain a rather large number of particles, since they are striking predominantly at some considerable distance from the center. Figure 3 shows that on the average the particle number in a $C$ shower is of the order $10^6$, and for showers of this size the exponent of the number distribution is no longer close to the value $\gamma=1.5$ used in the

[12] A very similar corrected structure function has been used by Campbell and Prescott (reference 2) for the representation of their experimental burst size distribution.

calculation (see Williams,[1] Blatt[13]). In recompting the density distribution, changes in both $\gamma$ and $f$ were therefore allowed, and the best agreement as shown in Fig. 5(c) was obtained with $\gamma=1.7$ and the value of $\epsilon$ given above.

It should be stressed as a remarkable result that, while for all three groups corrections of the structure function were found necessary, these corrections vary only slightly over a wide range of shower sizes: $C$ showers, with an average initial energy of $8\times10^{15}$ ev (for single-photon origin), gave $\epsilon=0.15$; $B$ showers, initiated on the average by photons of $7.1\times10^{14}$ ev, have $\epsilon=0.20$, and $A$ showers with an average initial energy of $9.1\times10^{13}$ ev show $\epsilon=0.24$. Expressed in terms of the "age parameter" $s$, a variation of the shower energy by a factor 100 corresponding to a change in the value of $s$ according to shower theory from about 1 to 1.3, yields a variation in the exponent of the density distribution near the core by only 0.09.

### (2) Multiple Cores

Since in the primary collision the electron-producing particles are ejected with a considerable multiplicity, the existence of multiple shower cores with an angular separation of the order $10^{-4}$ radian in the observation system has long been suspected. Each of the cores represents a higher concentration of energy than its surroundings, and in traversing the lead absorber of the arrangement should appear as a singularly dense "local cascade." At the observation level, the separation between these multiple cores may be of the order of the dimensions of the core-analyzing set. Consequently, it can be expected that occasionally a multiple-core structure should be found.

Local cascades of energies between $10^9$ and $10^{10}$ ev are frequently observed, and even events with more than one local core are not particullarly rare. A typical case is reproduced in Fig. 6. Although it is not at all certain that these events are directly related to the shower-initiating collision it appeared tempting to make an attempt to correlate the characteristic features of those cascades—in particular their angular separation for a given cascade energy—with the shower energy $E_0$.

It is then necessary to set a lower limit for the energies of the local cascades to be included in the analysis, and to classify the events according to their energies. For the cloud chamber pictures, the depth of the cascade maximum rather than the number of particles at the maximum was chosen as the criterion for classification, since the local cascades were usually too dense to permit an accurate count of the particle number. Pairs or groups of local cores were included in the survey if none of the cascades had passed the maximum in the fourth shelf, and at least one of them reached the maximum only in the fifth shelf or lower. The events were then grouped according to the depth of the cascade maxima of the two local cores, expressed in the number of lead plates traversed: a "7-plates event" is one in which one local cascade reaches its maximum under the third plate, the other under the fourth plate. The classification indicates, therefore, directly the total energy present in the two local cores.

33 cases with local-core structure were found. Within the limits of these rather poor statistics, the relative frequencies were about the same for all shower types

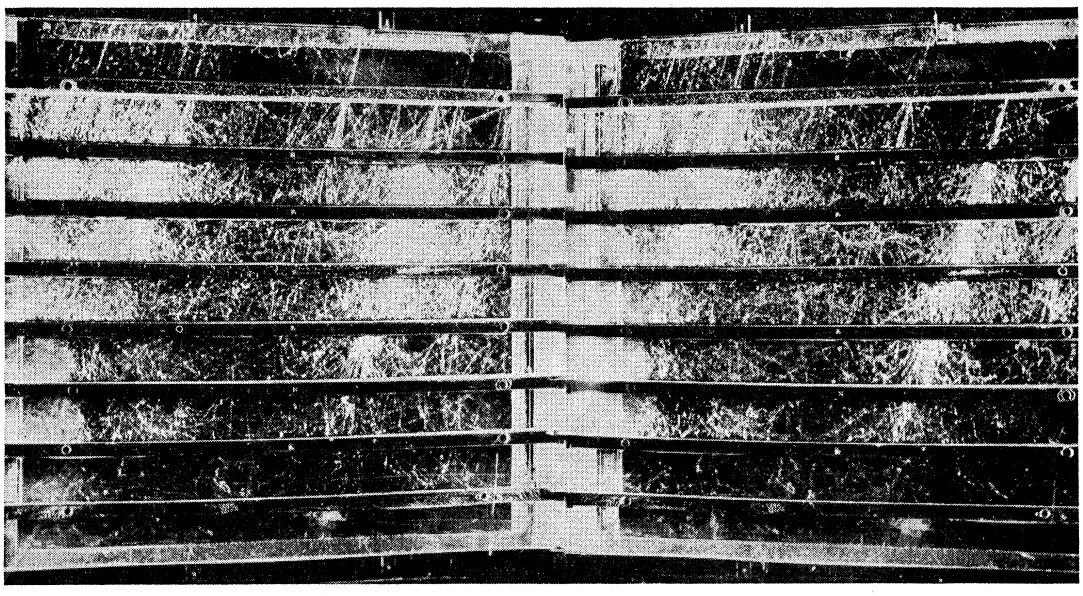

FIG. 6. Cloud-chamber photograph of an event with several "local cores."

[13] J. Blatt, Phys. Rev. **75**, 1584 (1949).

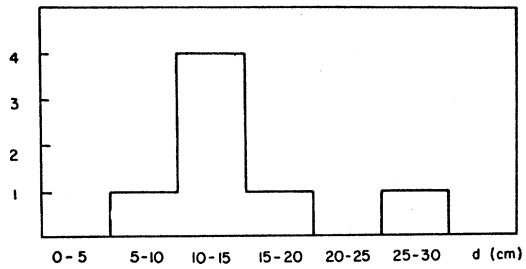


FIG. 7. Histogram of the separations $d$ of $B$-shower local cores with maxima under less than eight lead plates.

and certainly not markedly higher for $C$ showers as one might expect because of the smaller angular separation of the initial secondaries. Actually, the frequency of the events was in good agreement with the expected rate of high-energy electrons and photons if the flattening of the energy spectrum in the core area is taken in account. All the cascades observed started in the first lead plate or in the upper chamber wall.

Next it had to be determined whether for a given shower type, and for a given energy group of the local cascade, the separation of the two cores is fairly representative of the event. This seems to be so; for instance, the distribution of the distances $d$ between the axes of the two cascades of the "7-plates" and "8-plates" group of $B$ showers is reproduced in Fig. 7 and shows that it is meaningful to ascribe an average distance $\langle d\rangle = 14.9$ cm to the group. Similar results were found for the other groups.

It must be emphasized that the average distance in the chamber thus determined, should not be mistaken for the true average separation between the cascades. The latter could only be construed after due corrections for the finite size of the analyzing set, and this can only be done on the basis of specific assumptions about the theory of nuclear collisions: that is, assumptions otherwise avoided in this paper. On general grounds, however, one will expect the angular separation to decrease with increasing $E_0$, and such a variation might also be expected for the separation observed in this experiment.

If now the average distances of the various groups of local-core events are compared for the three shower types, one finds a very slight increase of the separation with the total energy of the local cascades, but no significant variation with the shower energy. This result is shown in the histogram of Fig. 8. From these data it appears that the local cores are not directly related to the primary collision and do not demonstrate the multiplicity of the initial interaction. However, it should be stressed again that the assumption underlying this analysis—that even without the corrections necessary to reduce the data obtained to the true angular separations, these experimental data will exhibit a distinct variation with $E_0$—is somewhat uncertain and difficult to prove. The possibility that the observations reported in this section are essentially determined by instrumental causes can therefore not be excluded.

For the hodoscope pictures, a clear recognition of all multiple electron-core events is not possible; chance configurations resulting in a structure resembling that of a local electron cascade may easily occur with a frequency comparable to that of genuine multiple cores, in particular in the denser showers. Nevertheless a strong energy dependence of the separations might perhaps be found from the comparison of the frequency of such apparent groups with that of single "background" clusters. The result of a survey was again negative: no difference between the three shower groups could be observed.

## IV. THE PENETRATING COMPONENT

### (1) Mean Free Path and Composition of the Nucleonic Component

Although several measurements of the abundance of penetrating particles in air showers have been reported (e.g., Ise and Fretter,[8] Sitte,[14] Greisen *et al.*,[15] McCusker,[16] and Hodson[17]), their lateral distribution has not yet been carefully investigated. Since in particular the distribution and relative frequency of $N$ particles near the shower core would demonstrate a possible variation with the primary energy of the fractional energy transfer into the electron-producing component, the analysis of the present experiment was extended to include a study of the penetrating component.

All attempts to analyze the penetrating shower component into its two main constituents, $N$ particles and $\mu$ mesons, are based on the identification of the nuclear collisions initiated by the first, and on the

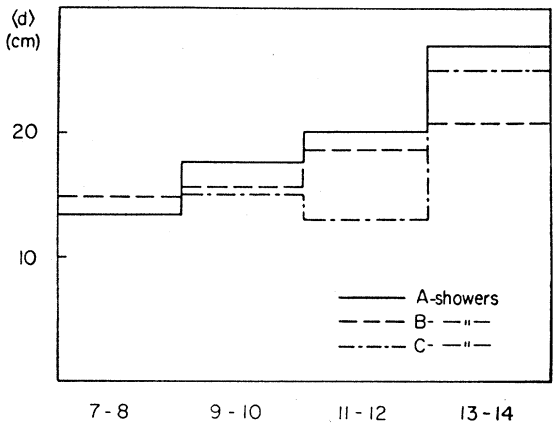


FIG. 8. Histogram of the average separation $\langle d\rangle$ of local cores of various energies.

[14] K. Sitte, Phys. Rev. **78**, 721 (1950); **87**, 351 (1952).
[15] Greisen, Walker, and Walker, Phys. Rev. **80**, 535 (1950).
[16] C. B. A. McCusker, Proc. Phys. Soc. (London) **A63**, 1240 (1950); C. B. A. McCusker and D. D. Millar, Proc. Phys. Soc. (London) **64**, 915 (1951).
[17] A. L. Hodson, Proc. Phys. Soc. (London) **A66**, 65 (1952).

subsequent correction for the cases in which the nucleons failed to interact. Here, obviously, the definition of an identified nuclear collision is rather arbitrary, and the more or less stringent conditions imposed in the various experiments probably account for the sometimes conflicting results of different investigators. Furthermore, in order to apply the corrections for the escaping $N$ particles, their interaction mean free path must be known, and its value is dependent on the choice of a certain type of collision for identification of the $N$ component. Thus, for instance, if local showers of high penetration and multiplicity are required, a "geometrical" mean free path is certainly correct if the measurement is confined to the identification of nucleons of high energy; but contributions from less energetic nucleons which may still in some cases—and hence with a longer mean free path—initiate equally large showers[6] would not be correctly estimated.

Consequently, it was deemed advisable to redetermine independently the mean free path of the interactions chosen in the analysis of the present experiment. Of course it is also preferable to relax the conditions of complexity and penetration of the local interactions so as to include low-energy collisions. The suitable limit is determined by the resolution of the experimental method, and hence not exactly the same for cloud chamber and hodoscope. This point will be discussed later; the determination of the interaction mean free path was based on cloud chamber evidence only. In this case, local interactions were identifiable if either at least one charged penetrating secondary was ejected accompanied by at least one heavy track, or more than one heavily ionizing particle was observed, or a single scattering of more than 10 degrees.

A survey of the distribution among the various lead plates of the origins of nuclear interactions may easily introduce a systematic error, because of the difficulty of identifying a nuclear event against a background of high electron density. If in a part of any one shelf the recognition was deemed uncertain, a corresponding volume in all shelves was excluded from the survey, in order to avoid biasing against the region near the maximum of the electron transition effect. From the location of the observed showers, the total number $N_0$ of incident $N$ particles can then be calculated even without the knowledge of the mean free path $\lambda$ [see Eq. (3) in reference 6], and with it the fractions $N_x/N_0$ of particles which escaped interaction under a layer $x$ g/cm² can be determined. Since $N_x/N_0 = \exp(-x/\lambda)$, the interaction mean free path is directly obtained from a logarithmical plot as in Fig. 9. The data obtained are compatible with the assumption of a geometrical cross section ($\lambda = 165$ g/cm²), and this value was therefore adopted for all subsequent calculations.

A very rough study of the ratio of neutral and charged $N$ particles was also performed. For this purpose, events could be included independent of their location,

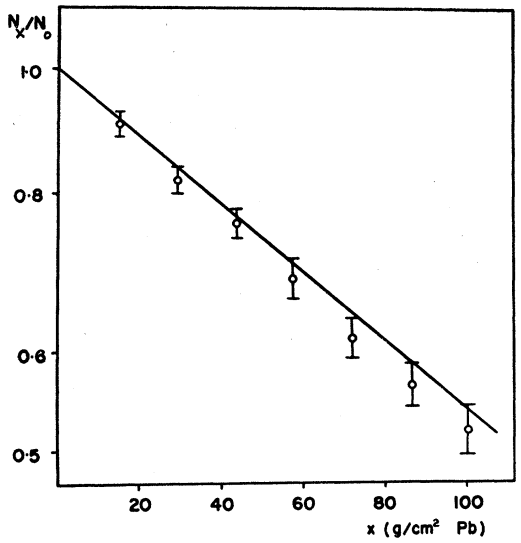


FIG. 9. Ratio $N_x/N_0$ of $N$ particles which escaped interaction in $x$ g/cm² of Pb, as a function of the thickness $x$ (from cloud-chamber data). The solid line is the distribution calculated with a mean free path of 165 g/cm².

but all those cases were omitted where the nature of the shower primary appeared doubtful because of a possible obliteration of its track by the electron shower. Thus, only 64 events were classified; among them were 26 neutron-produced showers. Accordingly, the neutron component can be estimated as (41±8) percent of all $N$ particles in the shower. In the following, a neutron/proton ratio of 0.8 will be used, in agreement with this analysis and with earlier determinations.[14,15]

### (2) Abundance and Abundance Ratio

Both cloud-chamber and hodoscope pictures permit only a classification of the penetrating component into "interacting" and "noninteracting" particles. If, instead, one wishes to group them rather into "$N$ particles" and "$\mu$ mesons"—taking the customary view that these two categories comprise at least the bulk of the penetrating shower particles—it should be remembered that the "noninteracting" particles include also all the charged $N$ particles which failed to interact, and that a corresponding number of unobserved neutrons has to be added to the total.

As to corrections for chance coincidences of a soft shower with independently incident penetrating particles, with fast coincidence circuits and with reasonably good cloud chamber technique, only the contribution of single mesons traversing the cloud chamber during its resolving time is of importance. The latter, however, is quite considerable even if mesons travelling at more than 10° from the shower direction are excluded. Fortunately, this good angular resolution is possible as long as the showers are observed near the core. The necessary correction was, therefore, obtained and checked in two ways: by calculating it with the best

TABLE I. Relative abundance and abundance ratio of penetrating particles in air shower cores.

| Composition | Events | *A* showers | *B* showers | *C* showers |
|---|---|---|---|---|
| $\frac{\mu \text{ mesons}}{\text{electrons}}(\%)$ | Cloud chamber | 0.93±0.17 | 0.83±0.12 | 0.80±0.19 |
| | Hodoscope | 0.81±0.10 | 0.86±0.12 | 0.73±0.09 |
| | Average | 0.86±0.08 | 0.85±0.07 | 0.74±0.07 |
| $\frac{N \text{ particles}}{\text{electrons}}(\%)$ | Cloud chamber | 0.68±0.12 | 0.50±0.09 | 0.46±0.12 |
| | Hodoscope | 0.58±0.10 | 0.60±0.07 | 0.41±0.06 |
| | Average | 0.63±0.08 | 0.56±0.06 | 0.43±0.06 |
| $\frac{N \text{ component}}{\text{Penetrating particles}}(\%)$ | | 0.43±0.05 | 0.40±0.04 | 0.37±0.05 |
| $\frac{\text{Penetrating particles}}{\text{electrons}}(\%)$ | | 1.51±0.12 | 1.41±0.09 | 1.17±0.09 |

estimate for the resolving time of the chamber (0.15 sec), and by counting the number of randomly traversing single mesons in pictures taken with the same cloud chamber and at the same altitude, but with a different triggering system in which the initiating event was clearly defined,[6] just as it was done for the electron component. The results of both methods were in fair agreement, and the tables below give the number of $\mu$ mesons after correction for the chance traversals.

In the analysis of the hodoscope pictures, events were classified as penetrating if at least one counter was discharged in all four trays, and in such a way that a particle path could reasonably be reconstructed. Thus, a few events with a straggling soft-particle cascade continuing down to the lowest tray were disregarded. On the other hand, it may be noticed that the penetration condition (a total of 8-in. Pb+$\frac{1}{2}$-in. Fe) is slightly more stringent than that usually imposed upon the hard component. But in view of the flat range spectrum of the $\mu$-meson component the difference is not of significance.

Events were counted as due to $N$ particles if a penetrating shower was found, i.e., an event containing at least two discharged counters in at least two successive levels, with a separation of at least one space between the counters triggered in each level. Events were registered as due to noninteracting particles if a single counter was discharged in each of the shielded trays, or a small group of neighboring counters in one level together with single counters in the adjacent level or levels (knock-on showers).

A summary of the results of the analysis of the penetrating events as observed both in cloud chamber and hodoscope is given in Table I. The abundance of the components is given in percentage of the electron density, and in each case the cloud chamber and hodoscope data are shown separately as well as their average. In general, they agree fairly well; a possible slight difference in the relative frequency of $N$ particles may be due to the different minimum energies recognized. The errors shown include statistical standard deviations and possible mistakes in the classification of doubtful events; the effect of the uncertainties in the values of the parameters used for correction (mean free path and neutron/porton ratio) was not included. While these uncertainties would affect the results in a systematic way, their possible influence is small compared with the predominant statistical errors and certainly is of no weight in the discussion of the results.

The most essential features of the results shown in Table I are:

(a) The relative abundance of $\mu$ mesons near the shower core does not vary significantly with the shower size. Within the limits of the experimental errors, its value is the same as that observed in other shower experiments were the detection system was not as strongly biased in favor of shower cores.

(b) The relative abundance of $N$ particles seems to increase slightly with decreasing shower energy, or with increasing shower age. Similarly, the ratio of the number of all penetrating particles to that of the electrons undergoes a slight change: showers of lower energy contain slightly more penetrating particles than those of higher energy. The difference is mostly due to the $N$ component; the $\mu$-meson fraction remains practically constant.

## V. CONCLUSIONS

From the results of the two preceding sections, several conclusions can be drawn.

(i) The electron distribution near the core is considerably flatter than that predicted by the Molière theory. It is also not in agreement with the structure function of an "old" shower initiated by a single particle. This is demonstrated by two facts: the deviation found for $C$ showers is much larger than it could be expected for single-particle initiated cascades in the neighborhood of their maximum development, and furthermore, the differences between the three groups of showers are smaller than those predicted for showers of so widely different energies, under the assumption of a single initiating particle. As it has been pointed out above, it was thought futile, at this stage, to attempt to fit the experimental data by a corrected theoretical distribution based on multiple production of $\pi^0$ mesons in the initial collision. However, the general features of the electron distribution near the core, as observed in this

experiment, may be of help in a future more extensive study.

(ii) It is tempting, though still highly speculative, to consider some basic ideas in an attempt to understand the remarkable insensitivity of the structure function with regard to shower size. Three interpretations may be suggested.

The simplest and perhaps most conventional assumption explains this independence as a result of the continuing replenishment of the electronic shower component by the electron-producing secondaries of the nucleon cascade. This replenishment "rejuvenates" the shower and tends to wipe out age differences. But this explanation would require a considerable effect of the "source function" representing the coupling between the nucleon cascade and the electron cascade—an effect which, so far, has been treated as very small.

Secondly, one might try to interpret the similarity in the core structure of all showers, together with the apparent absence of a genuine multiple-core structure representative of the primary interaction, in terms of the energy spectrum of the particles ejected in the first shower-initiating collision. These facts would then suggest a spectrum of the Fermi type[18] rather than of the Heisenberg type.[19] The former predicts a distribution peaked at some medium energy value, and fairly well approximated by the assumption that all secondaries carry the same energy. Since the average multiplicity increases with the primary energy $E_0$, the average—and representative—secondary energy rises slower than with the first power of $E_0$. Heisenberg's theory, on the other hand, while it also predicts a slow increase with $E_0$ of the *average* secondary energy, permits a greater share of high-energy secondaries which would reflect in more typical features of the cores of high-energy showers.

Lastly, one might choose the radical interpretation that, in spite of their difference in particle numbers (and hence presumably in their initial energies), the three groups of showers do not differ appreciably in their average age, but are all observed near the cascade maximum and, accordingly, must have originated at various depths in the atmosphere. Such an interpretation would necessitate major revisions of the customary picture of air showers, but certain observations reported by Piccioni and Cool[20] lead to very similar conclusions.

(iii) The abundance of penetrating particles near the core, summarized in Table I, is not significantly different from that previously reported in other experiments where detection of showers striking nearby was not made a stringent requirement, and where consequently the average distance of the apparatus from the shower axis was larger. Over a considerable region the abundance ratio varies, therefore, only very slowly if at all with the distance from the axis. Since the distribution of the heavier penetrating particles, unlike that of the electrons, is essentially determined not by multiple scattering but by their angular spread at production, and since the core represents the region of highest average energy as well as that of highest particle density, this result suggests that the processes through which, in the nuclear interactions, the energy is distributed among the various shower components do not vary appreciably with energy. This extends the conclusions reached in an earlier experiment.[21]

(iv) The slight difference between the three shower groups in the composition of the cores can easily be understood in terms of the age of the showers. In this connection the decrease of the abundance of penetrating particles, and especially of the $N$ component, with increasing shower energy deserves attention. This decrease demonstrates that the nucleonic cascade reaches its maximum at greater depth than the electronic component, and shows that the frequently reported proportionality between these two components[14–17,20] has only a limited range. This proportionality has usually been interpreted as a proof of the genetic relation between the two cascades, and it can be understood equally well if it is assumed, in the customary way, that the nucleonic cascade produces the electrons or if the nucleons are considered as secondary to the electronic component (Cool and Piccioni[22]).

The discrepancy between the increase in the $N$ component/electron ratio reported here, and the constant values found in the earlier experiments, is probably due to the arbitrariness in the instrumental selection of the $N$ particles. In the present experiment, it was attempted to set the low-energy limit of the recorded nuclear interactions as low as possible, and $N$ particles were registered that might not have been identified in other experiments. A considerable fraction of the nucleons in air showers is in an energy range where the degree of inelasticity of the nuclear interactions depends rather sensitively on the energy. These particles, while continuing the propagation of the nucleonic component, will not contribute much to meson production and hence will not transfer an appreciable amount of energy to the electronic cascade.

The experiment was made possible through the use of the facilities of the Inter-University High Altitude Laboratory at Echo Lake, Colorado, and the authors wish to express their thanks to Professor Byron E. Cohn and Professor Mario Iona, Jr., of the University of Denver for their cooperation. In preparing and running the experiment, Dr. E. M. Harth and Mr. F. E. Froehlich have given valuable assistance. Part of the funds required were obtained under a contract with the U. S. Atomic Energy Commission.

[18] E. Fermi, Progr. Theoret. Phys. (Japan) **5**, 510 (1950); Phys. Rev. **81**, 583 (1951).
[19] W. Heisenberg, *Z.* Physik. **126**, 569 (1949).
[20] O. Piccioni and R. L. Cool, Phys. Rev. **91**, 433 (1953).
[21] K. Sitte, Phys. Rev. **87**, 351 (1952).
[22] R. L. Cool and O. Piccioni, Rochester Meeting on High Energy Physics, December, 1950; Phys. Rev. **82**, 356 (1951).

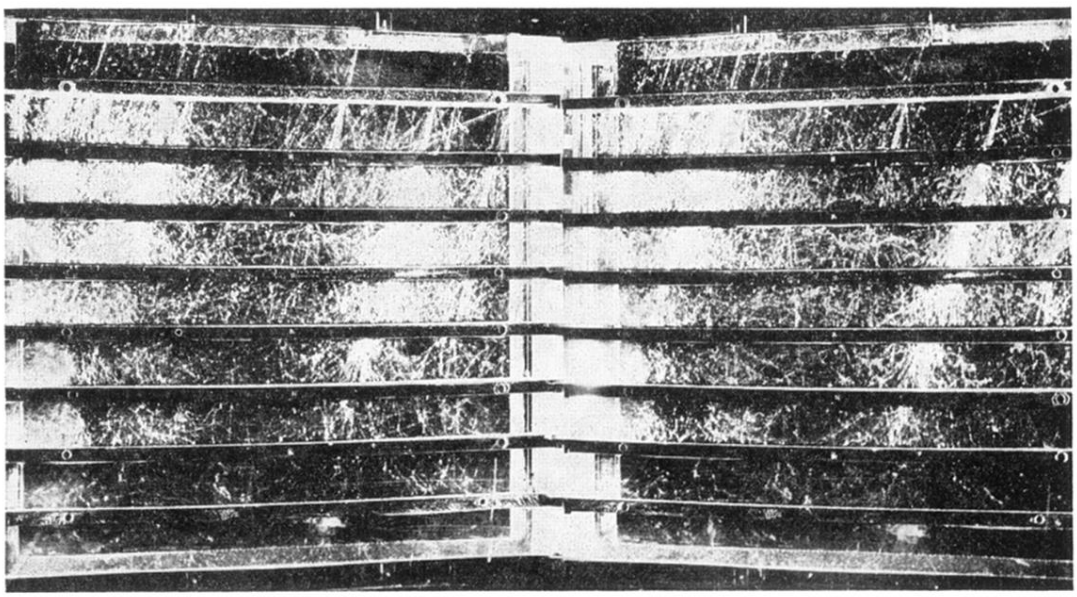

FIG. 6. Cloud-chamber photograph of an event with several "local cores."